

Optimizing the Parameters of a Quasi-Static Magnetic Field Generator using GAPSO

Wubing Zhu, Wenchun Zhao*, Jinwu Zhuang, Shengdao Liu and Guohua Zhou

College of Electrical Engineering, Naval University of Engineering, Wuhan, 430033, China

*Email: zhaowenchun1973@hotmail.com

Abstract — A homogeneous magnetic field is widely used in different research fields, and the homogeneity and accessibility of the designed magnetism space must be carefully studied. In this paper, three component coil models are setup with different configurations. By using the Genetic Algorithm Particle Swarm Optimization (GAPSO), the parameters (currents and location) of the symmetrical distributed coils are successfully optimized. Numerical calculations and simulations demonstrate that the optimized parameters can meet the requirements of homogeneity and accessibility. Taking the practical installation precision of coils into account, the optimized parameters are slightly adjusted, and the homogeneity (more than 99%) was improved to meet the requirement. In terms of the quasi-static field generator, alternating currents (AC) applied to the coils with optimized parameters produced the required changing uniform magnetic field. The design is verified by simulations with a Finite Element Method (FEM) software Flux3D.

Keywords - homogeneous magnetic field, accessibility, quasi-static magnetic field generator, GAPSO

I. INTRODUCTION

Steel naval vessels produce a magnetic field signal when sailing in water. This signal has been a reliable and stable source for mine and aerial magnetic field detectors, both of which impact the safety and effectiveness of naval vessels [1, 2]. The magnetism produced by the vessels can be classified in three ways: a permanent magnetic field (PM), an induced magnetic field (IM), and an eddy current magnetic field (EM). Research on the PM and the IM has matured enough to control them [2], while the EM requires further study. When vessels roll, yaw, or pitch in the water (at frequencies less than 5 Hz), an EM is produced due to the changing magnetic flux [3] through the vessels. In the fields of ship degaussing and shipboard high-precision magnetic field measurement [4], one of the primary interference sources is the unavoidable EM caused by wind, waves, or ship manipulation. This interference could also restrict the development of magnetic silencing techniques.

To measure the EM accurately, a dynamic magnetic field must be created in the space where the EM measurement experiment is performed. The homogeneity and frequency of the transient magnetic field can influence the measured EM. Recently, because of the different application requirements in various research fields such as medical science [5], agriculture [6], and space industries [7], a series of developments have been achieved for the design of magnetic field production. However, a special quasi-static magnetic field generator for measuring the EM of naval vessels should meet the design requirements in both homogeneity and accessibility. Herein, Genetic Algorithm-Particle Swarm Optimization (GAPSO) is applied to optimize the physical parameters of the coils to create the required generator.

In Section 2, the overall design scheme of the generator is introduced. In Section 3, the method for calculating the magnetic field of a finite-length straight conductor is deduced, which provides the basis for the coil parameter optimal models construction. In Section 4, coil optimization models for each direction of the generator are constructed. Then, each specific example of an optimization model is solved with the GAPSO algorithm and verified by simulations with the FEM software Flux3D [8] in Section 5. In Section 6, a method for quasi-static magnetic field production for the measurement of EM is proposed and the proposed method is verified by simulations with Flux3D.

II. THE OVERALL DESIGN SCHEME OF THE MAGNETIC FIELD GENERATOR

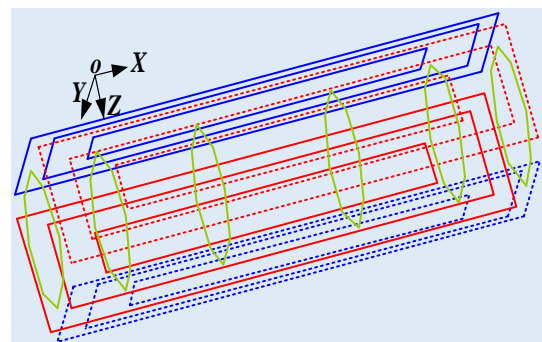


Figure 1. The overall design scheme of the magnetic field generator

Several points should be particularly noted when designing the magnetic field generator: (1) the dimensions of the space coils, (2) the accessibility to the region of the uniform magnetic field, and (3) the homogeneity of the

region of the required uniform magnetic field. As shown in Fig. 1, considering the three points above and the space restrictions for EM measurements in our laboratory, a series of octagonal coils are used to form a longitudinal system (X-coils). For the sake of accessibility and easy installation, the transverse coils (Y-coils) and vertical coils (Z-coils) are constructed with planar coils that can produce a uniform magnetic field effectively [9].

III. THE MAGNETIC FIELDS ANALYSIS OF A FINITE-LENGTH STRAIGHT CONDUCTOR

As stated in Ref.[10], the local and the integral approaches can be selected to design coils, and the advantages and drawbacks have been demonstrated clearly there. For the design of the magnetic field generator in Section 2, the integral method is more suitable. Without losing the accuracy of the magnetic field calculation in volume of interest (VOI), assuming that all the turns of each winding contribute equally to the total magnetic flux density, and the current filament method is opted to calculate magnetic field caused by the coils system [10]. The calculation of the magnetic field of a finite-length straight conductor at an arbitrary field point, which can be applied to calculate the magnetic field of any closed electrified coil according to the superposition theorem, is the basis of the construction of the optimal coil model. As shown in Fig. 2, for a current-carrying straight conductor ending at $A(a_0, a_1, a_2)$ and $B(b_0, b_1, b_2)$, the field components at $P(x_0, y_0, z_0)$ are shown to be [11],

$$h_x = h_1 \frac{s_x}{\sqrt{s_x^2 + s_y^2 + s_z^2}} \quad (1)$$

$$h_y = h_1 \frac{s_y}{\sqrt{s_x^2 + s_y^2 + s_z^2}} \quad (2)$$

$$h_z = h_1 \frac{s_z}{\sqrt{s_x^2 + s_y^2 + s_z^2}} \quad (3)$$

where,

$$\begin{aligned} h_1 &= \frac{I}{4\pi a} (\cos \theta_1 - \cos \theta_2) \\ &= \frac{I}{4\pi a} \left(\frac{d_3^2 + d_1^2 - d_2^2}{2d_3d_1} + \frac{d_3^2 + d_2^2 - d_1^2}{2d_3d_2} \right); \\ d_3 &= \sqrt{(b_0 - a_0)^2 + (b_1 - a_1)^2 + (b_2 - a_2)^2}; \\ d_2 &= \sqrt{(b_0 - x_0)^2 + (b_1 - y_0)^2 + (b_2 - z_0)^2}; \\ d_1 &= \sqrt{(a_0 - x_0)^2 + (a_1 - y_0)^2 + (a_2 - z_0)^2}; \\ a &= d_1 \sin \theta_1; \\ s_x &= (z_0 - a_2)(b_1 - a_1) - (y_0 - a_1)(b_2 - a_2); \end{aligned}$$

$$\begin{aligned} s_y &= (x_0 - a_0)(b_2 - a_2) - (z_0 - a_2)(b_0 - a_0); \\ s_z &= (y_0 - a_1)(b_0 - a_0) - (x_0 - a_0)(b_1 - a_1). \end{aligned}$$

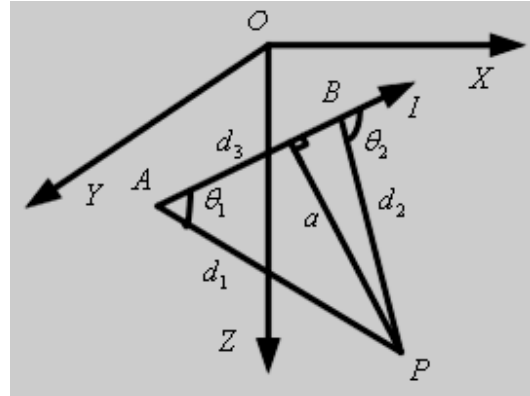


Figure 2. A random linear lead in space with electrical current

IV. THE CONSTRUCTION OF THE COIL OPTIMIZATION MODELS

A. Homogeneity in the volume of interest (VOI)

The homogeneity of the magnetic field reflects the variation of the magnetic field within the volume of interest (VOI). In references [12, 13], which used the magnetic induction at the central point of the coil system as the reference value, the variation of the magnetic flux density at the investigated points in space within the VOI is defined as the homogeneity of the magnetic flux density. However, the definition of homogeneity above does not provide global information about the homogeneity within the VOI.

Therefore, another definition of homogeneity proposed in Ref.[10], ε , a single global index that summarizes the maximum variation of the magnetic field magnitude within the VOI with respect to its mean value, is introduced to describe the homogeneity of the whole VOI, and the advantage of such a definition of homogeneity also has been explained. In fact, taking the homogeneity of the VOI into account can better optimize the parameters of the magnetic field generator, which would be beneficial to the EM measurement. For instance, the homogeneity of the X-component magnetic flux intensity can be calculated as

$$\varepsilon_x = 1 - \frac{|B_x|_{\max} - |B_x|_{\min}}{|B_x|} \quad (4)$$

where $|B_x|_{\max}$ and $|B_x|_{\min}$ are the maximum and minimum absolute values of the B_x within the VOI, respectively. Thus, ε_x is defined as the maximum change of the magnitude of magnetic flux density with respect to the mean value of the magnitude of B_x within VOI.

B. Three-component coils optimization models

For the longitudinal coils (X-coils), the free parameters of the n pairs of octagonal coils are the radius of the circumcircles L_i the distance to y-o-z plane d_i and the electric current LI_i . The transverse coils (Y-coils) are constructed from k pairs of rectangular coils with the free parameters, the sides of the rectangle Ta_i and Tb_i , the distance to x-o-z plane Th_i , and the electric current TI_i . For the vertical coils (Z-coils) constructed by l pairs of rectangular coils, the sides of the rectangle are Va_i and Vb_i , the distance to x-o-y plane is Vh_i , and the electric current is VI_i . In this work, each optimal model maximizes the homogeneity of the VOI as the target function, and the three optimal objective functions are expressed as,

$$f_x(L_1, \dots, L_n; d_1, \dots, d_n; LI_1, \dots, LI_n) = \max(\varepsilon_x) \quad (5)$$

$$f_y(Ta_1, \dots, Ta_k; Tb_1, \dots, Tb_k; Th_1, \dots, Th_k; TI_1, \dots, TI_k) = \max(\varepsilon_y) \quad (6)$$

$$f_z(Va_1, \dots, Va_l; Vb_1, \dots, Vb_l; Vh_1, \dots, Vh_l; VI_1, \dots, VI_l) = \max(\varepsilon_z) \quad (7)$$

V. THE DESIGN EXAMPLE AND VERIFICATION FOR COILS SYSTEM

In this paper, we took the application characteristics of the EM measurement of mock-up systems and the conditions of our laboratory into account. Therefore, several factors listed below were relevant in the optimization procedure to obtain the required design parameters.

(1) The available space in the laboratory can be expressed as $4.2m \times 4.2m \times 4.2m$. The coil dimensions should satisfy these installation requirements. The dimensions of the X-coils are restricted to a maximum radius of $2m$ and a maximum distance to the y-o-z plane of $2m$. The dimensions of the Y-coils are restricted to a maximum rectangle side-length of $4m$ and a maximum distance to the x-o-z plane of $2.1m$. The Z-coils' dimension restrictions are the same as that of the Y-coils. Coils intersection can be avoided by the dimensional restrictions above.

(2) The maximum power from a constant current source (CCS) restricts the current magnitudes' range in each current-carrying coil to be between $[-1000A, 1000A]$.

(3) The economic efficiency is another important factor. Consequently, the number of pairs of X-coils, Y-coils, and Z-coils cannot exceed 5.

(4) The uniformity of the X-coil, Y-coil, and Z-coil systems must meet the criteria: $\varepsilon_x, \varepsilon_y, \varepsilon_z \geq 95\%$.

A. Introduction of PSO

In fact, many optimization algorithms, such as GA, PSO, GAPS0, and TABU search algorithm, can be applied to obtain the optimal design parameters of the magnetic field generator. In this paper, the particle swarm optimization (PSO) algorithm [14] is used. PSO is a stochastic optimization technique based on population that initializes the particles randomly in the available solution range and speed range to stochastically search for the solution to the problem. Because the conventional PSO algorithm frequently displays premature and weak convergence, an advanced algorithm—GAPS0 [4], that overcomes these limitations is applied to compute the solutions of the optimization models. In Ref.[4] completed by our group, the GA, PSO and GAPS0 algorithms were used to solve the magnetic parameters for removing the ship's interference magnetism, and the GAPS0 algorithm has been proved to be more suitable than GA and PSO algorithms there. Herein, the GAPS0 algorithm is used to optimize the parameters of coils, also the optimized procedures and results obtained by the GAPS0 algorithm would be compared with that of the conventional PSO algorithm.

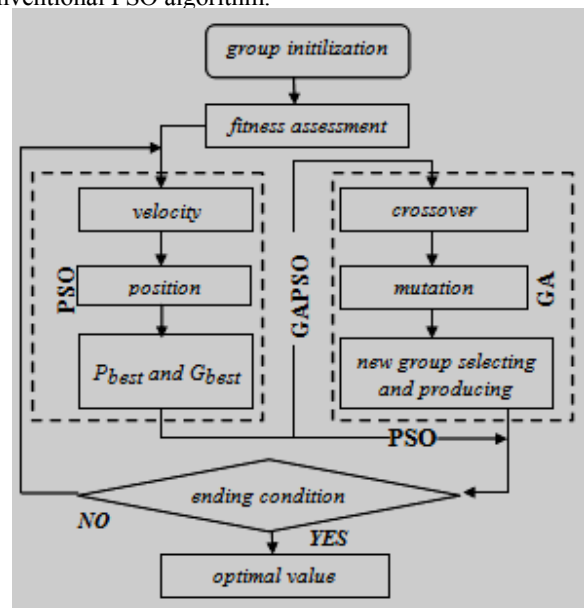


Figure 3. The flow chart of GAPS0 and PSO algorithm

Flow charts of the conventional PSO and GAPS0 algorithms are displayed in Fig. 3, the difference between the two algorithms above is that the conventional PSO do not integrate with the GA operation after P_{best} and G_{best} updating. The GAPS0 algorithm can be implemented according to the steps of GAPS0 in Ref.[4], parameters for PSO part are $c_1 = c_2 = 1.49445$, $\omega_{max} = 0.1$ and

$\omega_{\min} = -0.1$. For parameters of GA algorithm part, $lenchrom = 10$, $pc = 0.7$ and $p_m = 0.3$.

B. Results, discussion and verifications

Parameters of X-coils, Y-coils, and Z-coils have been optimized by the GAPSO algorithm and PSO algorithm, the convergent procedures for the X-coils, Y-coils, and Z-coils of the two algorithms above as shown in Fig. 4. Homogeneities optimized by the GAPSO algorithm is more acceptable with less convergent steps than the conventional PSO. Homogeneities of X-coils, Y-coils, and Z-coils calculated by coils parameters obtained from GAPSO result in 99.89%, 99.608%, and 99.608%, respectively. All the optimized parameters optimized by GAPSO algorithm are displayed in Tab. 1–3. XI1–XI5 denote the current parameters (Unit, A) of the five X-coils, and the electric currents are anticlockwise (seen from positive direction of the x-axis). Xd1–Xd5 represent the distances (Unit, m) between the octagons and the y-o-z planes. Similarly, YI1–YI5, Ya1–Ya5, Yb1–Yb5, ZI1–ZI5, Za1–Za5 and Zb1–Zb5 denote the current and dimensional parameters of the five Y-coils and the five Z-coils.

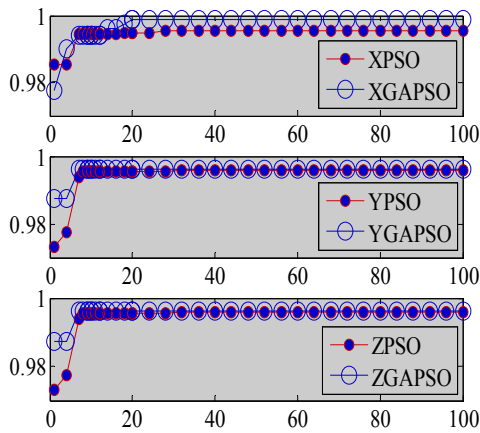


Figure 4. Parameters of the optimization procedures

TABLE I. OPTIMIZATION RESULTS AND ADJUSTED RESULTS OF X-COILS

XI1–XI5	(adjust) XI1–XI5	Xd1–Xd5	(adjust) Xd1–Xd5
-0.6121	-0.612	-0.382	-0.382
-0.75638	-0.756	-1.6903	-1.690
-0.34989	-0.350	-0.99039	-0.990
-1.3353	-1.335	-1.5404	-1.540
-0.22186	-0.222	-0.24621	-0.246

TABLE II. OPTIMIZATION RESULTS AND ADJUSTED RESULTS OF Y-COILS

YI1–YI5	(adjust) YI1–YI5	Ya1–Ya5	(adjust) Ya1–Ya5	Yb1–Yb5	(adjust) Yb1–Yb5
0.3584	0.358	-0.27326	-0.273	-0.11402	-0.114
-0.10642	-0.106	-0.10985	-0.110	-0.29128	-0.291
0.54356	0.544	-0.45487	-0.455	-0.64157	-0.642
0.50938	0.509	-1.2413	-1.241	-1.1544	-1.154
1.3073	1.307	0.64663	0.647	-0.54698	-0.547

ZI1–ZI5	(adjust) ZI1–ZI5	Za1–Za5	(adjust) Za1–Za5	Zb1–Zb5	(adjust) Zb1–Zb5
0.3584	0.358	-0.27326	-0.273	-0.11402	-0.114
-0.10642	-0.106	-0.10985	-0.110	-0.29128	-0.291
0.54356	0.544	-0.45487	-0.455	-0.64157	-0.642
0.50938	0.509	-1.2413	-1.241	-1.1544	-1.154
1.3073	1.307	0.64663	0.647	-0.54698	-0.547

TABLE III. OPTIMIZATION RESULTS AND ADJUSTED RESULTS OF Z-COILS

ZI1–ZI5	(adjust) ZI1–ZI5	Za1–Za5	(adjust) Za1–Za5	Zb1–Zb5	(adjust) Zb1–Zb5
0.3584	0.358	-0.27326	-0.273	-0.11402	-0.114
-0.10642	-0.106	-0.10985	-0.110	-0.29128	-0.291
0.54356	0.544	-0.45487	-0.455	-0.64157	-0.642
0.50938	0.509	-1.2413	-1.241	-1.1544	-1.154
1.3073	1.307	0.64663	0.647	-0.54698	-0.547

However, it is impossible to construct a magnetic field generator with the parameters above because of the precision limits of manual installation. Therefore, parameters were adjusted slightly and the adjusted parameters (labeled with adjust \times) are also displayed in Tab. 1–3. The homogeneity of the magnetic flux intensity of the X-coils, Y-coils, and Z-coils with the adjusted parameters are 99.98%, 98.72% and 98.67%, respectively; the adjusted parameters also satisfy the homogeneity requirements. To verify the accuracy and effectiveness of the coil parameter optimization, the magnetic flux intensity of the optimized coil system is also simulated with the FEM software Flux3D [8]. The magnetic flux intensity along a series of measured lines is used to verify the homogeneity of the VOI. The X-component magnetic flux intensity B_x of measured line 1 (from point (-500, 0, 0) mm to point (500, 0, 0) mm), the Y-component magnetic flux intensity B_y of measured line 2 (from point (0, -500, 0) mm to point (0, 500, 0) mm), and the Z-component magnetic flux intensity B_z of measured line 3 (from point (0, 0, -500) mm to point (0, 0, 500) mm) are computed to compare the optimized results and the simulation results. The homogeneity calculated by the optimization and simulation along each measure line is 99.708%, 98.72% and 98.72%, respectively. In Figs. 4–7, the X-component, Y-component, and Z-component of the magnetic flux intensity of the optimized results and the FEM simulation results of each measure line are displayed. The two results match so well that the plotted Flux datas are partially obscured by the markers used for the optimized data.

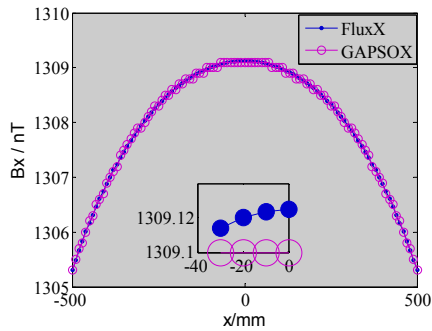


Figure 5. Comparison of B_x of measured line 1

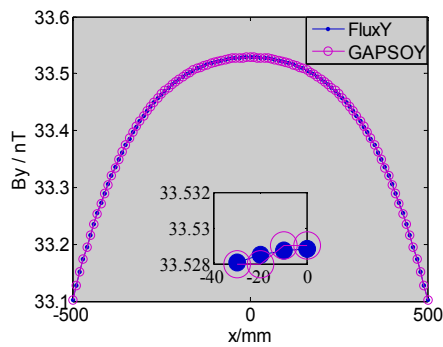


Figure 6. Comparison of B_y of measured line 2

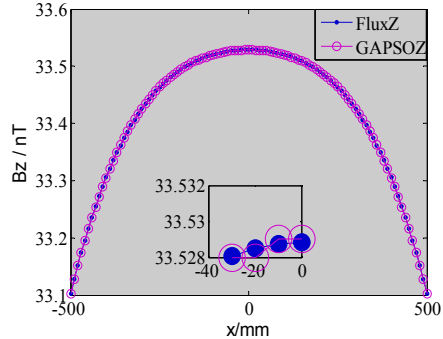


Figure 7. Comparison of B_z of measured line 3

VI. DESIGN OF THE QUASI-STATIC MAGNETIC FIELD GENERATOR

The time-harmonic equation with the magnetic vector potential \vec{A} can be expressed as [16],

$$j\omega\sigma\vec{A} + \nabla \times (\mu^{-1}\nabla \times \vec{A}) = \vec{J}^e \quad (8)$$

The magnetic flux intensity of a field point can be calculated using the Biot-Savart Law [16],

$$\vec{B} = \nabla \times \vec{A} = \nabla \times \frac{\mu_0 I}{4\pi} \int \frac{ds}{R} \quad (9)$$

For the quasi-static magnetic field case, the magnetic flux intensity of a field point from multiple sources can be

obtained by (8) and (9), and definitions of relevant variables (ω , σ , μ , \vec{B} and so on) can refer to Ref. [16]. In this paper, ACs are applied to coils to produce the quasi-static magnetic field. The angular frequencies of the motions of naval vessels are typically less than $10\pi \text{ rad/s}$, which is low enough to justify the use of the above method to calculate the magnetic field. The functional form of the currents switched on in the X-coils is $I_i \sin(\omega_i t + \varphi_i)$ where I_i is the adjusted current parameter in Tabs. 1–3, ω_i is $10\pi \text{ rad/s}$, and φ_i is zero. The calculated (labeled with GAPSOX) and simulated (labeled with FluxX) X-component magnetic flux intensity B_x at the point $(0, 0, 0)$ from $0s$ to $0.2s$ (one period) are displayed in Fig. 7. The B_x at $t = 0.05s$ from point $(-500, 0, 0)mm$ to $(500, 0, 0)mm$ is shown in Fig. 10 (labeled with Xmag). The functional form of the currents with switched-on Y-coils and Z-coils are the same as that of the X-coils. The calculated (labeled with GAPSOY) and simulated (labeled with FluxY) Y-component magnetic flux intensity B_y and calculated (labeled with GAPSOZ) and simulated (labeled with FluxZ) B_z at point $(0, 0, 0)$ within $[0, 2s]$ are shown in Fig. 8 and Fig. 9. B_y at $t = 0.05s$ from point $(0, -500, 0)mm$ to the point $(0, 500, 0)mm$ is displayed in Fig. 10 (labeled with Ymag). Similarly, Z-component magnetic flux intensity B_z at $t = 0.05s$ from point $(0, 0, -500)mm$ to point $(0, 0, 500)mm$ is displayed in Fig. 10 (labeled with Zmag). Numerical and simulation results demonstrate that the GAPSO can be applied to design the quasi-static field exposure successfully.

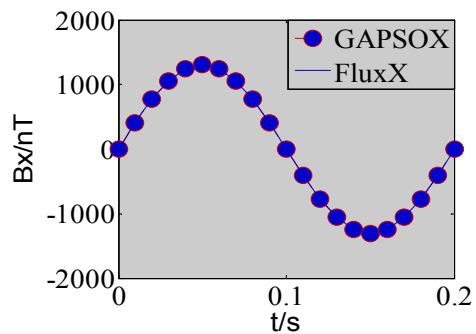


Figure 8. Comparison of optimization results of B_x

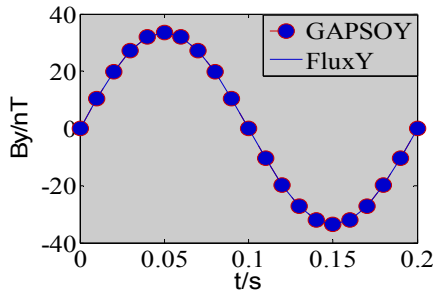


Figure 9. Comparison of optimization results of B_y

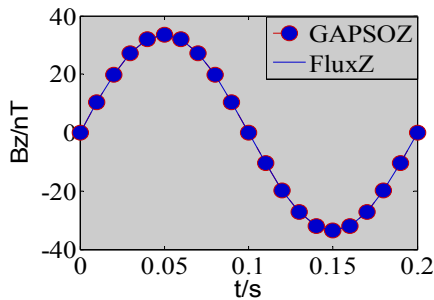


Figure 10. Comparison of optimization results of B_z

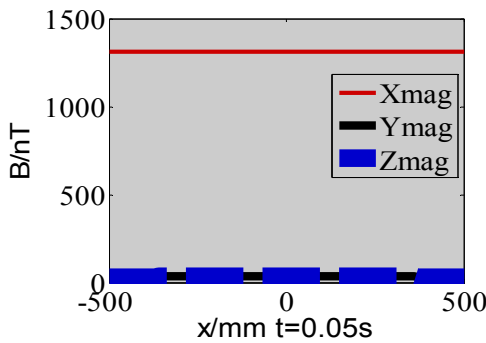


Figure 11. B simulations results with Flux along measured line

VII. CONCLUSION

In this paper, X-coil, Y-coil, and Z-coil optimization models of a magnetic field generator are constructed with different proposals. The GAPSO optimization algorithm is applied to obtain the design parameters for the coils of the static magnetic field generator. Based on the optimal design, the quasi-static magnetic field generator is successfully designed. Numerical calculations and simulations with Flux3D demonstrate that the amplitudes of the magnetic flux intensity of the quasi-static field generator and that of the static magnetic flux intensity are the same. The designed magnetic field generator can satisfy the requirements for EM measurement. In future work, a quasi-static magnetic field generator will be constructed in the laboratory to measure the EM of naval vessels, and the related numerical calculations of the EM will also be extended.

ACKNOWLEDGMENT

This work is supported in part by National Natural Science Foundation of China under grant No. 51377165 and No. 41476153.

REFERENCES

- [1] J. J. Holmes, *Exploitation of a Ship's Magnetic Field Signatures (Synthesis Lectures on Computational Electromagnetics)*, San Rafael, California: Morgan and Claypool Publishers, 2006.
- [2] J. J. Holmes, *Reduction of a Ship's Magnetic Field Signatures (Synthesis Lectures on Computational Electromagnetics)*, San Rafael, California: Morgan and Claypool Publishers, 2008.
- [3] Floch. Y. Le, C. Guérin, X. Brunotte and G. Meunier, "3-D computation of magnetic anomaly due to a rotating plate in the earth magnetic field," *IEEE Trans. Mag.*, vol. 38, no. 2, pp. 553-556, 2002.
- [4] J. J. Gao, X. L. Zhu, W. B. Zhu, "Accurate calculating method of marine three-component geomagnetic field in shipboard measurement," *Chinese Automation Congress*, IEEE Press, Nov. 2015, pp. 1504-1507, doi:10.1109/CAC.2015.7382738.
- [5] D. Cvetkovic, and I. Cosic, "Modelling and design of extremely low frequency uniform magnetic field exposure apparatus for in vivo bioelectromagnetic studies," *29th Annual International Conference of the IEEE on Engineering in Medicine and Biology Society*, IEEE Press, Aug. 2007, pp. 1675-1678, doi:10.1109/IEMBS.2007.4352630.
- [6] M. A. Azpurua, Y. Sanchez, and E. J. Paez, "A homogeneous magnetostatic field exposure system for presowing magnetic treatment of seeds," *PIERS Draft Proceedings*, Aug. 2013, pp. 1438-1442.
- [7] C. Gu, S. N. Zou, T. M. Qu, J. Y. Ling and Z. H. Han, "Design of HTS coil for magnetic driving spacecraft," *IEEE Transactions on Applied Superconductivity*, vol. 20, no. 3, April 2010, pp. 997-1000, doi:10.1109/TASC.2009.2039929.
- [8] Flux, Cedrat. Meylan, France [Online]. Available: www.cedrat.com
- [9] I. Sasada and Y. Nakashima, "Planar coil system consisting of three coil pairs for producing a uniform magnetic field," *Journal of Applied Physics*, 99, 08D904, pp. 1-3, 2006, http://dx.doi.org/10.1063/1.2165107.
- [10] M. A. Azpurua, "A semi-analytical method for the design of coil-systems for homogeneous magneto-static field generation," *PIER B*, vol. 37, 2012, pp. 171-189, doi:10.2528/PIERB11102606.
- [11] Z. Yu, C. H. Xiao, Y. Z. Zhou and H. Wang, "The calculation of the magnetic field produced by an arbitrary shaped current-carrying wire in its plane," *Applied Mechanics and Materials*, vol. 756-759, 2013, pp. 3687-3691, doi:10.4028/www.scientific.net/AMR.756-759.3687.
- [12] V. Ogay, P. Baranov and A. Stepankova, "Modelling coils system for generating homogeneous magnetic field," *IOP Conf. Ser. Mater. Sci. Eng.* 66 012009, vol. 66, 2014, doi: http://dx.doi.org/10.1088/1157-899X/66/1/012099.
- [13] J. Wang, S. X. She and S. J. Zhang, "An improved Helmholtz coil and analysis of its magnetic field homogeneity," *Review of scientific instruments*, vol. 73, no. 5, 2175-2179, April 2002, doi: http://dx.doi.org/10.1063/1.1471352.
- [14] J. Kennedy and R. C. Eberhart, "Particle swarm optimization," *Proc. IEEE International Conference on Neural Network*. Perth, Australia, 1995.
- [15] S. Mohammad, T. Mona, S. Iman and A. Amir, "Minimum-time open-loop and closed-loop optimal guidance with GAPSO and neural fuzzy for samarai MAV fight," *IEEE Aerospace and Electronic Systems Magazine*, vol. 30, no. 5, pp. 28-37, June 2015, doi:10.1109/MAES.2015.7119822.
- [16] Z. Haznadar, Z. Stih, *Electromagnetic fields, waves and numerical methods*, Amsterdam, NL, IOS Press, 2000.